

# Treatment Planning Technique Applying the Combined CT Imaging and Computational Fluid Dynamics (CFD) Analysis

K. Hemtiwakorn\*, N. Phoocharoen, Guest members,  
V. Mahasittiwat, and M. Sangworasil, Members

## ABSTRACT

Combined medical imaging with computational fluid dynamics (CFD) analysis was used to demonstrate and evaluate airflow in human nasal cavity. The processes of this study are segmentation, meshing, solving, and post-processing. Firstly, Mimic 10.01 software was used to segment the nasal cavity. Secondly, Pro-STAR/amm software was employed to generate trimmed mesh of 338,496 elements. Finally, computational grid model was imported to STAR-CD version 3.24 for numerical computation, and visualize the solution by post-processing. The results show the nasal airflow simulation in both normal and abnormal human noses. It can be seen that for the normal nose breathing, the velocity magnitude of airflow was greatest in a nasal valve area which is the narrowest area of the human nose. Also, the air flow commonly passes through the main nasal passage and middle meatus areas, and velocities in both sides are not different. For the abnormal nose of nasal septum deviation, the result showed that the velocity magnitude inside the narrowed left side is very high and greater than the right side about 50-90 percent. Therefore, combined CT data and CFD analysis is very useful for doctor to evaluate the physiology and phenomena of airflow inside the patient's nose. Rhinosurgery could be employed those technique for the preparing the rhinosurgical planning. Nevertheless, the experimental validation is not reported in this paper but will be published in the further publication. In conclusion, this study is the important beginning of an applied CFD analysis with medical imaging. CT imaging combines with CFD analysis could be useful for rhinologist as a nose function evaluation technique. CFD based on CT imaging could be applied as a tool for the treatment planning.

**Keywords:** CFD, Nasal airflow, Treatment planning

---

\* Corresponding author.

Manuscript received on December 25, 2009.,

K. Hemtiwakorn is with the Biomedical Engineering, Faculty of Engineering, King Mongkut's Institute of Technology Ladkrabang, Bangkok, Thailand.

*E-mail addresses:* hemtiwakorn@gmail.com (K. Hemtiwakorn)

## 1. INTRODUCTION

Nose is an upper part of the respiratory tract which is the opening of a human airway. Three main functions of nose [1] are filtering, smelling, and optimization temperature and humidity to the ambient air before going through the lung. Since, nasal cavity of human is very narrow and complicate, visualization of nasal cavity is very difficult. The major symptoms such as difficult breathing, loss of smell, or sinus infection can increase the resistance to flow [2], and also may be occur from the obstruction or nasal septum deviation. The methods of rhinomanometry, acoustic rhinometry, or medical imaging, such as CT or MRI, can help the doctor to diagnose the pathology in human nose, and treatment planning. However, previous methods can not demonstrate the function of nose, such as airflow, in normal or abnormal case. CFD based on CT imaging and simulation software is the useful technique to evaluate the airflow direction, velocity, and pressure inside the nasal cavity for pre and post operations. The combination of medical imaging technique, such as CT or MRI, and computational fluid dynamics (CFD) analysis could be applied for the diagnosis, treatment planning, and evaluate the physiology of the nose after operation. Thus, this study proposed the combined CT imaging and CFD analysis as a tool help doctor for planning the nose operation.

## 2. NUMERICAL MODELING BASED ON CT IMAGING

### 2.1 GEOMETRIC MODEL CONSTRUCTION

The first process of this research is construction the geometric 3-dimensional nose model by using the computed tomographic (CT) data obtained from volunteer and segmentation software. DICOM data of CT images were imported into MIMICS 10.01 software (Materialize, USA) for segmenting the nasal airway excluded paranasal sinus. A threshold level range of about -1024 to -188 was applied to the area consisting of air. After automatic segmentation with threshold level of brightness, the manual segmentation should be performed not only in axial images but also in coronal and saggital images as shown in Fig.1.

Finally, 3-dimensional nose model was reconstructed as demonstrated in Fig.1.

## 2.2 COMPUTATION MESH GENERATING

The mesh generating software called Pro-STAR/amm software (CD-Adapco, UK) was used for this purpose. Unstructured mesh was generated in this study. Also, it is necessary to create at least two cell layers immediately next to the inner boundary of the 3-dimension model to obtain a stable and convergent solution. Therefore, two layers were located near to the wall. Fig.2 shows the trimmed-cell mesh with two layers cell structure near the model surface.

## 2.3 FLUID DYNAMICS CONDITION/ GOVERNING EQUATION

Airflow inside a human nasal cavity is in a dynamic state. It decelerates and accelerates from a resting state during normal breathing. The air is considered as incompressible and Newtonian with constant fluid properties. A numerical solution of the mean flow requires resolving the mass and momentum conservation equations (the "Navier-Stokes equations") solved by STAR-CD are in Cartesian tensor notation [1] as follows:

$$\frac{\partial}{\partial x_j}(\rho \cdot u_j) = 0 \quad (1)$$

$$\frac{\partial}{\partial x_j}(\rho \cdot u_j \cdot u_i - \tau_{ij}) = -\frac{\partial p}{\partial x_j} \quad (2)$$

where  $x_i$  is the Cartesian coordinate ( $i = 1,2,3$ )

$u_i$  = absolute fluid velocity component in direction  $x_i$ ,

$p$  = piezometric pressure =  $p_s - \rho_0 g_m x_m$  where  $p_s$  is static pressure,  $\rho_0$  is reference density, the  $g_m$  are gravitational acceleration components and the  $x_m$  are coordinates relative to a datum where  $\rho_0$  is defined

$\rho$  = density

$\tau_{ij}$  = stress tensor components

Standard low Reynolds number two-equations  $k-\varepsilon$  model is the turbulence model applied in this study.

## 2.4 BOUNDARY CONDITION AND NUMERICAL CONTROL

The computational grid nose model was imported into the commercial CFD software package, STAR-CD 3.24 of Adapco, UK, which solve the finite volume. Discretization of the governing equations was conducted using a Mono Tone Advection and Reconstruction Scheme (MARS), which is a second-order accurate differencing scheme. Of all differencing schemes available in STAR-CD, MARS was chosen for its optimal sensitivity to the solution accuracy and skewness of the mesh structure [2]. The

Semi-Implicit Method for Pressure-Linked Equations (SIMPLE) algorithm [3] was used to manage the pressure-velocity coupling. To stabilize the solution, under-relaxation factors were used for all the basic variables (0.5 for momentum and turbulent equations and 0.1 for pressure). The sets of linearized and discretized equations for all variables were solved using the algebraic multigrid method for improving the calculation performance of trimmed meshes [2]. We assumed that the uniform velocity profile and the axial component of velocity were perpendicular to the flow inlet faces. The boundary conditions at the nostrils and the nasopharynx were set to the static pressure = 0 and outlet boundary face is fixed mass flow rate (kg/s). Turbulence intensity was set to 10% and the dissipation rate at the inlet boundaries was set with a dissipation length scale of 1 cm. Convergence was judged by monitoring the magnitude of the absolute residual sources of mass and momentum, normalized by the respective inlet fluxes. The iteration is continued until all above residuals fall below 0.001

## 3. INSPIRED NASAL AIRFLOW SIMULATION RESULTS

In this study, the normal breathing in human was studied in the first investigation. Next, the abnormal breathing during the pathology in the patient's nose was studied. Comparison between normal and abnormal breathing are useful for doctor to evaluate the patient status and treatment planning. The results of the airflow simulation in both normal and abnormal noses are demonstrated in the following.

### 3.1 NORMAL BREATHING IN HUMAN NOSE

Computer modeling was constructed using CT data obtained from a female patient. CT scanning was performed on a General Electric LightSpeed VCT (Wisconsin, USA) scanning station with the following parameters: 120 kVp, 200.0 mA, rotation time of 0.9 s, thickness 1.25 mm. To construct an anatomical 3-dimensional model of nasal cavity, 48 axial sections from a computed tomographic image of a single subject were used for the numerical modeling. The computations were performed using a personal computer with an Intel Core 2 Quad 2.4 GHz CPU and 6 GB of memory, which typically took 2 hours per run to complete.

The velocity magnitude of airflow in right nasal cavity is visualized in saggital view as shown in Fig 3. From this figure, it can be seen that the greatest velocity magnitude occurs in nasal valve area, because it is the narrowest area of the nose. Also, high values and variation of velocity magnitude appears in the anterior part of nasal airway in front of a turbinate region. The flow was slower when passed through the main nasal passage and turbinate regions because there were wider than the anterior part of the nasal

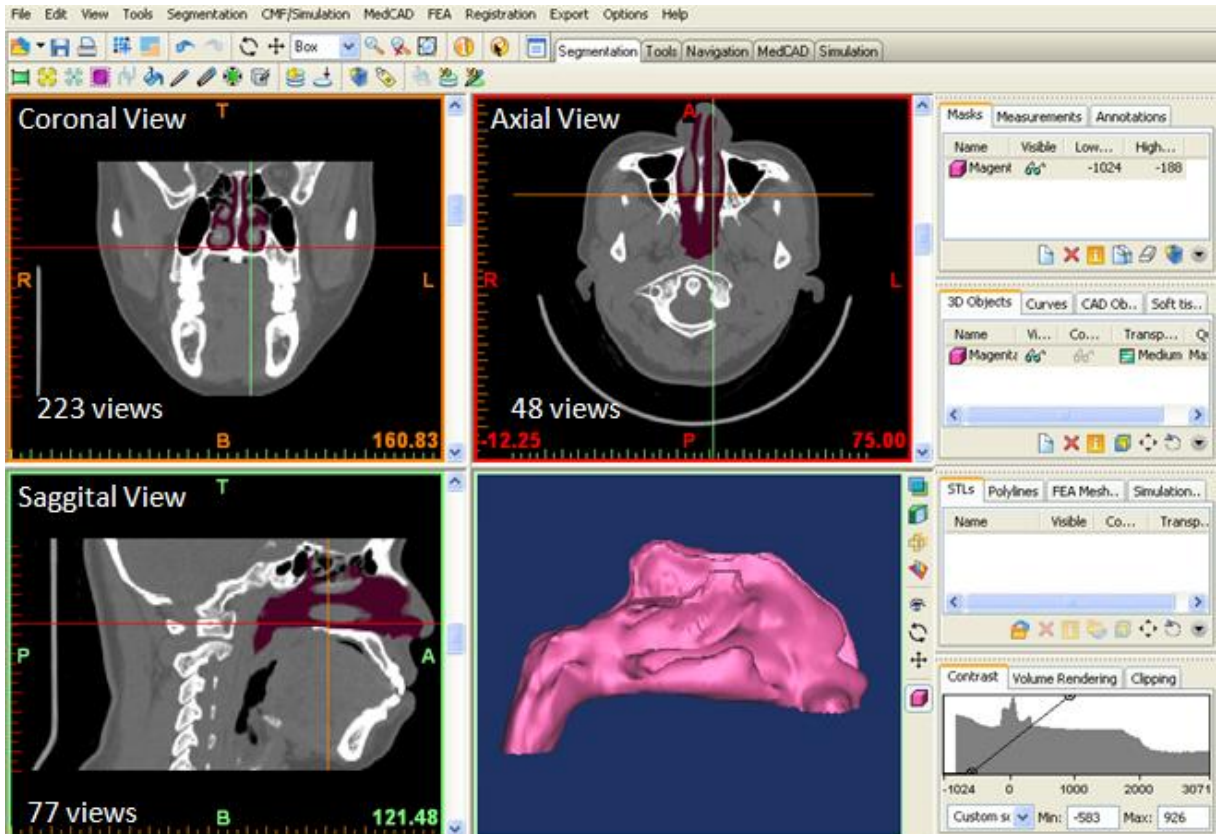


**Fig.1:** CT images in 3 planes of coronal, axial, and saggital were used for segmentation. Magenta color areas demonstrate a nasal airway (exclude paranasal sinus) after automatic and manual segmentations. 3D reconstructed nose model is shown in this figure.

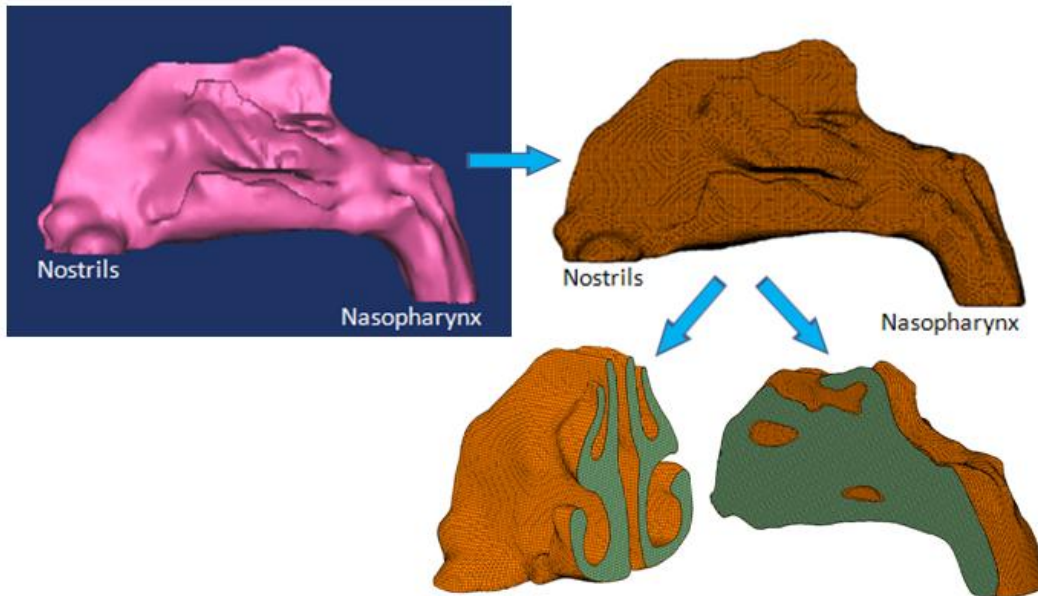


**Fig.2:** Trimmed cell mesh model was performed after constructing the 3D model obtained from CT images. Cross-sectional grid models in coronal and saggital planes are shown in this figure.

cavity. For the airflow in turbinate meatus region, almost flow pass through the middle meatus which is

wider than another meatus. Thus, slow flow passes through the inferior and superior meatus.

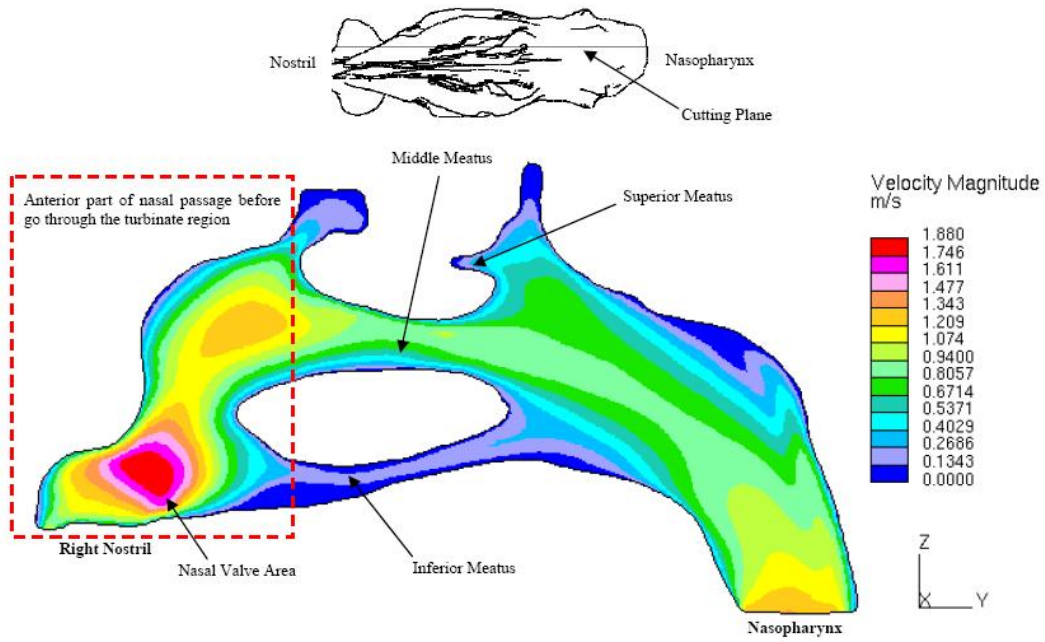
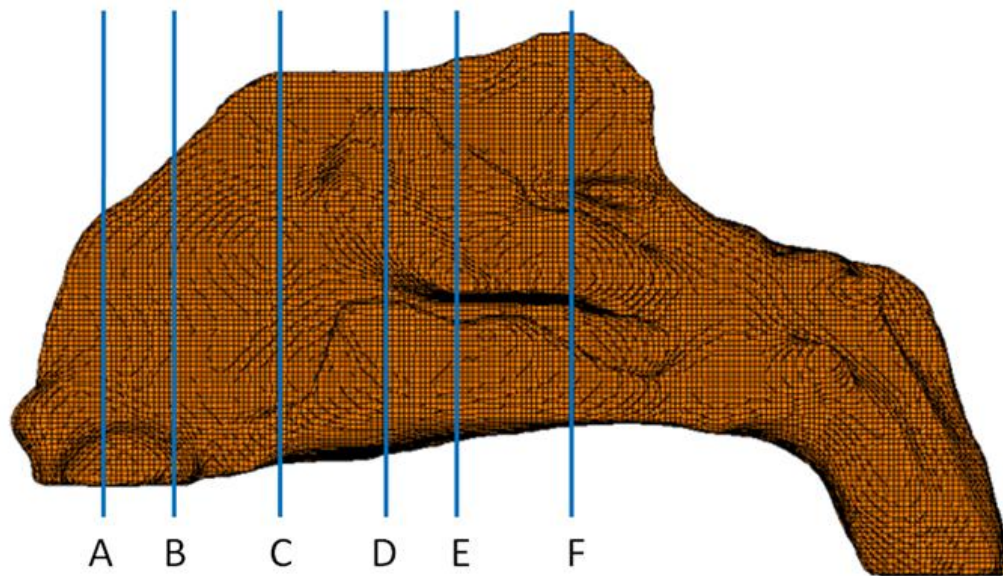


**Fig.3:** Velocity magnitude of the right nasal cavity is shown in a saggital plane. Landmark line of cutting plane location is demonstrated.



- Plane A is nostril
- Plane B is nasal valve area (narrowest area of nasal cavity)
- Plane C is head of inferior turbinate
- Plane D is beginning of middle turbinate,
- Plane E is middle portion of nasal turbinate, and
- Plane F is the beginning of superior turbinate nearly the end of nasal turbinate area

**Fig.4:** Coronal cutting planes of nasal model.

Moreover, cutting model in coronal plane to visualized velocity magnitude in specific regions was presented. The velocity magnitudes of airflow were demonstrated in six planes as shown in Fig.4. Plane

A is a nostril. Plane B represents the nasal valve area. Plane C is the head of inferior turbinate region. Plane D is the beginning of middle turbinate region. Plane E represents the middle part of nasal cavity,

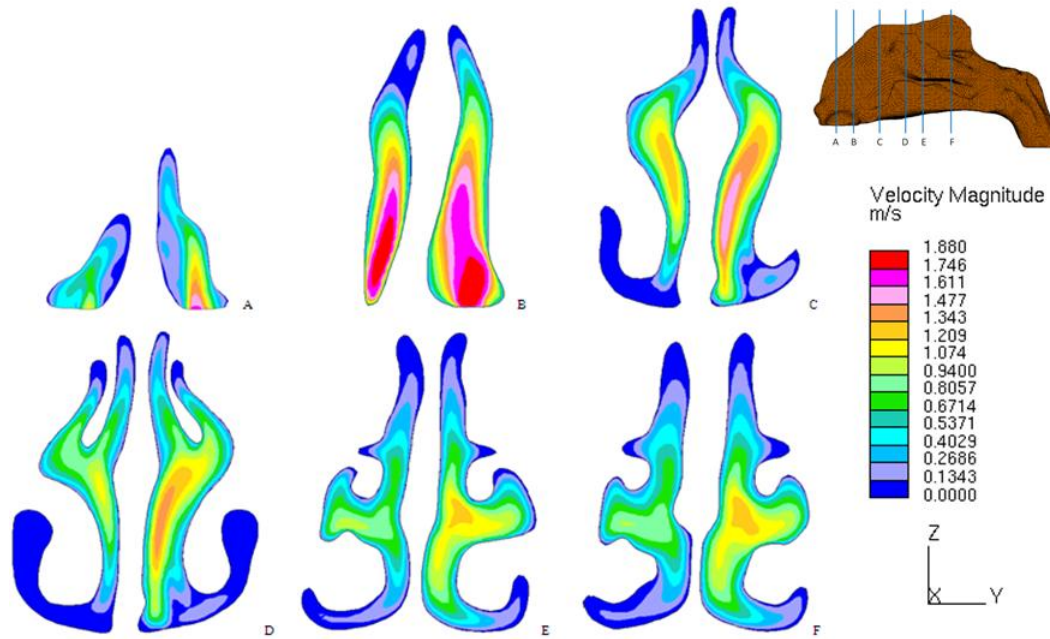


**Fig.5:** The velocity magnitude (m/s) of nasal airflow in each coronal plane (A-F) obtained from normal nose model.

and plane F is the beginning of superior turbinate region.

The velocity magnitudes in each plane are presented in Fig. 5. The results show that velocities increase immediately in the nasal valve area. The highest velocity magnitude of 1.88 m/s occurs in plane B which is the nasal valve area. Moreover, it can be seen that airflow commonly passes through the main nasal passage and the middle meatus. However, slow flow of 0.13-0.26 m/s appears in the inferior and superior meatus. From the Fig.5, it can be seen that flow commonly passed near the nasal septum more than diffused to the nasal wall.

### 3.2 ABNORMAL BREATHING IN DEVIATED NASAL SEPTUM

Computer modeling was constructed using CT data obtained from a male patient with the nose obstruction due to the nasal septum deviation. To construct an anatomical 3-dimensional model of nasal cavity, 64 axial sections from CT images of a single subject were used for the numerical modeling. From the CT data, the images show that nasal septum is deviated to the narrowed left side of patient's nose as shown in Fig 6. To confirm the diagnosis results of nasal septum deviation and narrowed left side, rhinoscan was performed in the same patient. The rhinoscan result shows that the left side is very narrow as compare with the right side as shown in Fig 7. Also, the inspired volume flow rate in a left side is lesser than a right side as 34.6 cm<sup>2</sup>/s and 219.3 cm<sup>2</sup>/s for left and right sides, respectively.



**Fig.6:** CT image obtained from a male patient of nasal septum deviation.

The first airflow simulation result in abnormal nose model is demonstrated in Fig 8. The figure shows the velocity magnitudes of airflow inside a nasal cavity with a deviated nasal septum and very narrow in the left side of nasal cavity. It can be seen that the velocity magnitudes of airflow inside the left nasal cavity are greater than the right side, particularly for the obstructive area approximately 1.5-2.0 m/s for a left side and 1.2 m/s for a right side, respectively. As comparing with the normal nose model shown in Fig. 5, it can be seen that the velocity magnitude of airflow

inside the both nasal cavities is not much difference.

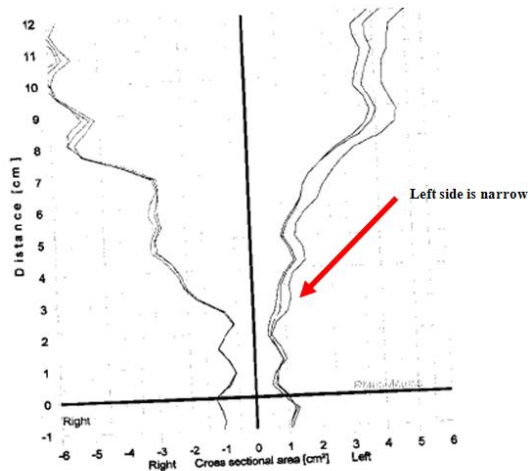


Fig.7 Rhinoscan result showed that a left side of nose is narrow.

**Fig.7:** Rhinoscan result showed that a left side of nose is narrow.

#### 4. APPLICATION OF CFD FOR A TREATMENT PLANNING

To correct the abnormal nasal cavity of the patient, treatment technique of surgery is an invasive technique but necessary particularly for the case used in this research. Therefore, preparation the surgical planning is very important. Combined CT data and CFD analysis is very useful for doctor to evaluate the physiology and phenomena of airflow inside the patient's nose. Doctor can understand the affect of abnormal nose geometry to the direction, velocity, and pressure of airflow inside the nose. Moreover, rhinosurgion could be applied those technique for the rhinosurgical planning, and also visualize the nasal airflow obtained from the process of pre-operation preparation. Nevertheless, nasal airflow obtained from pre-post operation can be calculated by a CFD technique but does not show in the present. Also, the experimental validation of nasal airflow simulation obtained from this study will be reported in the future publication.

#### 5. CONCLUSION

This study presents nasal airflow simulation in normal and abnormal adult noses by combining CT imaging with computational fluid dynamics (CFD) analysis. It enables us to study the physiology of nasal breathing. The advantage of this method is the airflow simulation on a realistic model derived from CT imaging. Moreover, combined CT data and CFD analysis is useful for doctor to diagnosis, evaluate the phenomena of airflow inside the patient nose, treat-

ment planning, and pre-post operative airflow simulation.

#### 6. ACKNOWLEDGMENT

The authors wish to acknowledge the facilities of computer and software provided by the Computer Service Center of King Mongkut's Institute of Technology Ladkrabang (KMITL), Bangkok, Thailand. Moreover, authors would like to thank Mahidol University and SWU, Bangkok, Thailand, for their supporting the CT images. We would like to thank Assoc. Prof. Manas Sangworasil for his kindly suggestion, support, and encouragement throughout this research. Finally, the author wish to thank the Office of the Higher Education Commission, Bangkok, Thailand for the financial support during this research.

#### References

- [1] Z.V.A. Warsi, Conservation form of the Navier-Stokes Equations in General Nonsteady Coordinates, AIAA Journal, 19, pp.240-242, 1981.
- [2] STAR-CD 3.2 Users' Guide. Computational Fluid Dynamics Ltd., 2004.
- [3] S.V. Patankar, D.B. Spalding. A Calculation Procedure for Heat, Mass and Momentum Transfer in Three-Dimensional Parabolic Flows. Int. J. Heat Mass Tranfer, 15, pp. 1778-1806, 1972.



**K. Hemtiwakorn** obtained her B.Sc and M.Sc in radiological technology in 2005 and 2008, respectively from the Mahidol University, Bangkok, Thailand. She is currently pursuing her Ph.D in biomedical engineering, Faculty of Engineering, Bangkok, Thailand. She also the research assistant in Ramathibodi Hospital in several research projects about radiological technology and applied biomedical engineering. Her research interests include computational fluid dynamics (CFD) in human body, biomechanics, and apply the CFD for evaluate and treatment planning in the ENT patient.



**N. Phoocharoen** obtained his B.Eng in Mechanical Engineering from King Mongkut's Institute of Technology Ladkrabang (KMITL), Bangkok, Thailand. He is currently pursuing his M.Eng in Mechanical Engineering, KMITL, Bangkok, Thailand. He has more than 10 years experience in CFD research in both mechanical and biomedical engineering. He is now the research assistant in the Computer Service Center, KMITL, Bangkok, Thailand.

KMITL, Bangkok, Thailand.

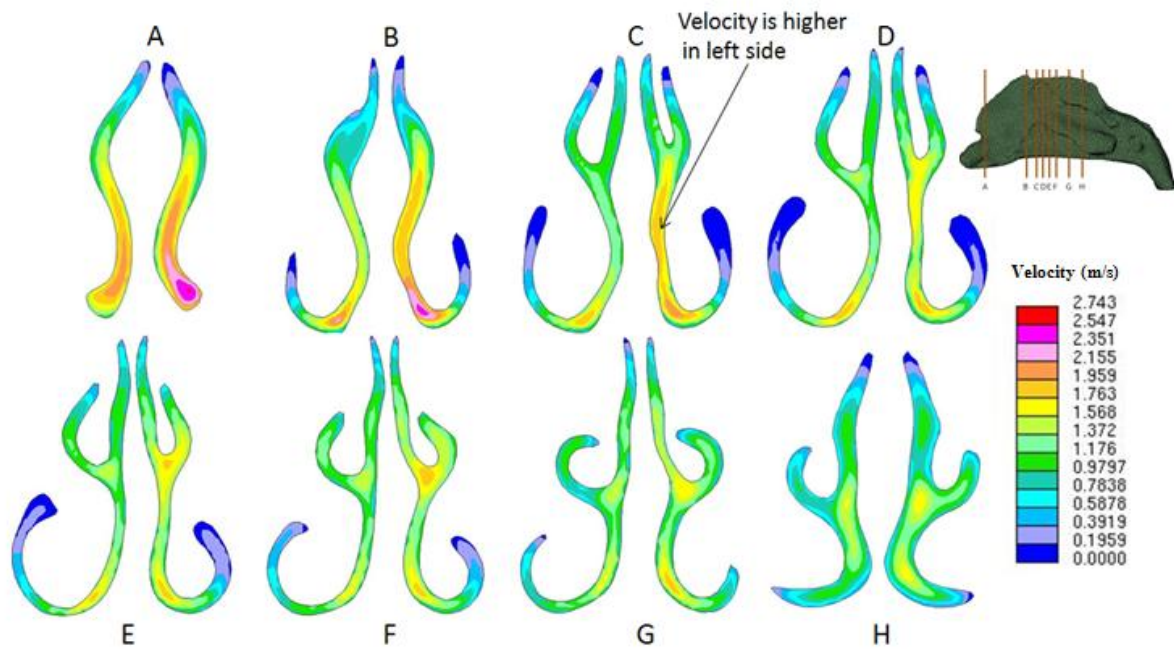


**Fig.8:** The velocity magnitude (m/s) of airflow inside the abnormal nose model of deviated nasal septum in each coronal plane (A-H).



**V. Mahasithiwat** obtained his MD from Prince of Songkla University (PSU). He is currently the ENT expert in Faculty of Medicine, Srinakharinwirot University. His research interests include ENT technology and development of earring aids, nose operation technique, and eye tracking.



**M. Sangworasil** was born in Bangkok, Thailand in 1951. He received the Bachelor of engineering and Master of Engineering from King Mongkut's Institute of Technology at Ladkrabang, Bangkok, Thailand in 1973 and 1977 respectively, and the D. Eng (Electronics) from Tokai University, Japan, in 1990. Following his graduate studies, he worked almost 28 years at Electronic Department, Faculty of Engineering, King Mongkut's

Institute of Technology at Ladkrabang, Bangkok where he is currently an associate professor. His research interest are in the area of image process with emphasis on Image Reconstruction, 3D modeling, Image Classification and Image Filtering.